Preprints of the 21st IFAC World Congress (Virtual)
Berlin, Germany, July 12-17, 2020

Observer-based LPV Control with Anti-Windup Compensation: A Flight Control Example

Julian Theis * **Nicolas Sedlmair** * **Frank Thielecke** *
Harald Pfifer **

* *Institute of Aircraft Systems Engineering, Hamburg University of Technology, Hamburg, Germany. (e-mail: {julian.theis, nicolas.sedlmair, frank.thielecke}@tuhh.de).*
** *Department of Mechanical, Materials and Manufacturing Engineering, University of Nottingham, Nottingham, UK. (e-mail: harald.pfifer@nottingham.ac.uk).*

Abstract: A low-complexity anti-windup compensation scheme for linear parameter-varying (LPV) controllers is proposed in this paper. Anti-windup compensation usually increases complexity of LPV controllers significantly. A synthesis algorithm is used in this paper that, unlike conventional algorithms, splits the problem into an observer synthesis and a subsequent state feedback synthesis. The resulting controller structure is exploited for a novel differential implementation that allows straightforward incorporation of conventional anti-windup logics. The method is used to design a pitch-axis flight control law for an unmanned aerobatic aircraft, where anti-windup compensation is an important practical requirement. Applicability is demonstrated in nonlinear simulation using a flight-test-validated high-fidelity model.

Keywords: linear parameter-varying control, control system synthesis, robust control, observers, mixed sensitivity problem, coprime factorization, flight control

1. INTRODUCTION

The dynamics of aircraft vary substantially with environmental conditions, in particular airspeed and air density. In conventional flight control, gain-scheduling is often used to acknowledge this dependence. Controllers are designed using linear techniques for a large number of different operating points in the entire flight envelope and the individual control laws are interpolated. This approach is time consuming and complex. Thus, research efforts were made during the 1980s and '90s to develop methods for a single, joint design over the entire envelope with controller adaptation taking place automatically. One control paradigm that arose in this context is linear parameter-varying (LPV) control. It can be understood as formalized gain-scheduling with an online adaptation to the current operating point. As of today, the framework is well developed with a large body of literature (Becker and Packard, 1994; Wu et al., 1996; Apkarian et al., 1995; Apkarian and Gahinet, 1995; Bennani et al., 1998) and mature computational tools (Hjartarson et al., 2015; Balas et al., 2015). Performance is specified in terms of the induced $\mathcal{L}_2$-norm, providing a natural extension of the widely popular $\mathcal{H}_\infty$-control framework. The present paper considers LPV systems whose state space matrices are arbitrary functions of the scheduling parameters. This is more general than LPV systems modeled via lower fractional transformations (LFT), for which the state space matrices must have a rational dependence on the scheduling parameters. For LPV systems with arbitrary parameter dependence, the most common way of obtaining controllers is solving a semidefinite program (SDP) over a gridded parameter space using the formulation of Wu et al. (1996). This approach has three practical issues: 1) The SDP scales badly with the number of state variables and scheduling parameters. 2) The controller depends explicitly on the time-derivative of the scheduling parameters. These parameter variation rates are often difficult to measure and are neglected in many application examples in the literature. 3) Including anti-windup compensation is far from trivial, even though solutions exist. In particular, methods usually result in an LPV anti-windup compensator that is as complex as the corresponding LPV controller (e. g. Lu et al., 2005; Prempain et al., 2009). A different approach is formulated by Wu et al. (2000), who introduce the saturation level as an additional scheduling parameter. This, however, aggravates the first two issues mentioned above.

Very recently, a novel synthesis algorithm for LPV controllers was proposed by Theis and Pfifer (2020). It is computationally less expensive than the state-of-the-art method and yields controllers that do not depend on the time-derivative of the scheduling parameter. In this paper, it is shown that the novel approach also enables simple and efficient anti-windup compensation that does not increase controller complexity. To this end, a differential implementation, inspired by the $\mathcal{D}$-implementation of Kaminer et al. (1995), is used. It implements the observer-based controller in a "differential" form, i. e., such that the derivative $\dot{u}$ instead of the control signal u is calculated. Such implementations are also referred to as velocity or incremental algorithms and have their roots in motor control, see e. g.

Åström and Hägglund (2006). The paper starts with a short review of preliminaries and the observer-based LPV controller synthesis in Section 2. The differential implementation of such observer-based controllers is developed in Section 3. The resultant form is then used in Section 4 to incorporate anti-windup compensation into the pitch-axis control law for a 25 kg unmanned aerobatic aircraft. Nonlinear simulations demonstrate the applicability of the proposed method.

2. PRELIMINARIES

2.1 Linear Parameter-Varying Systems

LPV systems are a class of dynamic systems whose state space representations depend continuously on a time-varying scheduling parameter vector $\rho\colon \mathbb{R} \mapsto \mathcal{P}$, where $\mathcal{P} \subset \mathbb{R}^{n_\rho}$ is a compact set of allowable parameters. Additionally, the parameter rates $\dot\rho\colon \mathbb{R} \mapsto \mathcal{Q}$ are restricted to lie in a polyhedron $\mathcal{Q} = \{\dot\rho \in \mathbb{R}^{n_\rho} \mid |\dot\rho_i| \leq \nu_i\ ,\quad i = 1, \ldots, n_\rho\}$. Hence, the set of all admissible parameter trajectories is $\mathcal{T} = \{\rho(t) \mid \rho(t) \in \mathcal{P} \wedge \dot\rho(t) \in \mathcal{Q} \quad \forall t \in \mathbb{R}\}$. A state space representation of an LPV system P with state $x(t) \in \mathbb{R}^{n_x}$, input $v(t) \in \mathbb{R}^{n_v}$, and output $y(t) \in \mathbb{R}^{n_y}$ is

$$\begin{bmatrix} \dot x(t) \\ \hline y(t) \end{bmatrix} = \left[\begin{array}{c|c} A(\rho(t)) & B(\rho(t)) \\ \hline C(\rho(t)) & D(\rho(t)) \end{array}\right] \begin{bmatrix} x(t) \\ \hline v(t) \end{bmatrix} \qquad (1)$$

where $A\colon \mathcal{P} \mapsto \mathbb{R}^{n_x \times n_x}$, $B\colon \mathcal{P} \mapsto \mathbb{R}^{n_x \times n_v}$, $C\colon \mathcal{P} \mapsto \mathbb{R}^{n_y \times n_x}$, $D\colon \mathcal{P} \mapsto \mathbb{R}^{n_y \times n_v}$ are continuous matrix functions. The performance of an LPV system can be specified in terms of its induced $\mathcal{L}_2$-norm

$$\|P\| = \sup_{v \in \mathcal{L}_2 \setminus \{0\},\ \rho \in \mathcal{T},\ x(0) = 0} \frac{\|y\|_2}{\|v\|_2}\ . \qquad (2)$$

The dependence on parameters and time is dropped where appropriate to shorten notation.

2.2 Mixed Sensitivity LPV Control

Throughout this paper, a standard unity feedback control loop with plant P and controller K is considered. The plant output is partitioned as $y = \left[\begin{smallmatrix} y_1 \\ y_2 \end{smallmatrix}\right]$, where y_1 are (integral-) controlled outputs and y_2 are additional feedback signals. Consequently, the control error is $e = \left[\begin{smallmatrix} y_{\text{ref}} - y_1 \\ -y_2 \end{smallmatrix}\right]$, where y_{ref} is a reference for y_1. The control signal is denoted u. The considered mixed sensitivity formulation characterizes performance as the induced $\mathcal{L}_2$-norm of the weighted closed-loop system shown in Fig. 1. The corresponding optimal controller synthesis problem is

$$\min_K \left\| \begin{bmatrix} W_e V_e^{-1} & 0 \\ 0 & W_u V_u^{-1} \end{bmatrix} \begin{bmatrix} S & SP \\ KS & KSP \end{bmatrix} \begin{bmatrix} V_e & 0 \\ 0 & V_d \end{bmatrix} \right\|, \qquad (3)$$

where $S = (I + PK)^{-1}$ denotes the output sensitivity function, cf. Skogestad and Postlethwaite (2005).

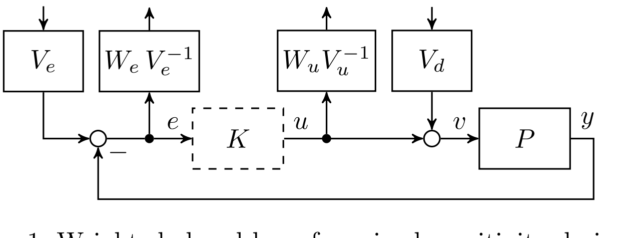

Fig. 1. Weighted closed loop for mixed sensitivity design.

Performance specifications are imposed through shaping filters W_e and W_u with state space realizations

$$\begin{bmatrix} \dot\xi_e \\ \hline z_1 \end{bmatrix} = \left[\begin{array}{c|c} 0 & B_{We}(\rho) \\ \hline C_{We}(\rho) & D_{We}(\rho) \end{array}\right] \begin{bmatrix} \xi_e \\ \hline \tilde e \end{bmatrix} \qquad (4a)$$

$$\begin{bmatrix} \dot\xi_u \\ \hline z_2 \end{bmatrix} = \left[\begin{array}{c|c} A_{Wu}(\rho) & B_{Wu}(\rho) \\ \hline C_{Wu}(\rho) & D_{Wu}(\rho) \end{array}\right] \begin{bmatrix} \xi_u \\ \hline \tilde u \end{bmatrix} . \qquad (4b)$$

A high gain in W_e dictates a sensitivity reduction and specifies tracking and disturbance rejection capabilities. An integrator in W_e enforces integral control. A high gain in W_u dictates a reduction in control effort. Hence, the weight W_u can enforce controller roll-off at high frequencies. The inputs to the dynamic weights W_e and W_u are a statically weighted control error $\tilde e = V_e^{-1}\, e$ and a statically weighted control effort $\tilde u = V_u^{-1}\, u$. The static weights V_e and V_u are tuning knobs. They can be selected based on the maximum allowable errors (V_e) and maximum allowable inputs (V_u). Thus, initial guesses are particularly easy. Similarly, V_d is a tuning knob for disturbance rejection that can be chosen based on maximum expected disturbances. For details about this parametrization see Theis et al. (2018, 2020).

2.3 Observer-based LPV Synthesis

Theis and Pfifer (2020) recently proposed a novel synthesis procedure that alleviates drawbacks of conventional LPV output feedback synthesis. The procedure uses the mixed sensitivity formulation (3) to solve for a structured observer-based LPV controller of the form

$$\begin{bmatrix} \dot\xi \\ \hline u \end{bmatrix} = \left[\begin{array}{c|c} A(\rho) + B(\rho)F(\rho) + L(\rho)C(\rho) & L(\rho) \\ \hline F(\rho) & 0 \end{array}\right] \begin{bmatrix} \xi \\ \hline e \end{bmatrix}, \qquad (5)$$

where L is an observer gain and F is a state feedback gain. The structure of the controller is depicted in Fig. 2. Its dynamic part, the observer O, is detailed in Fig. 3.

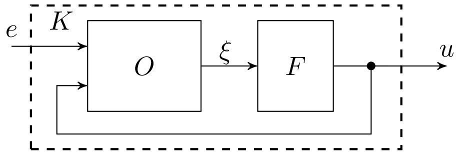

Fig. 2. Observer-based controller.

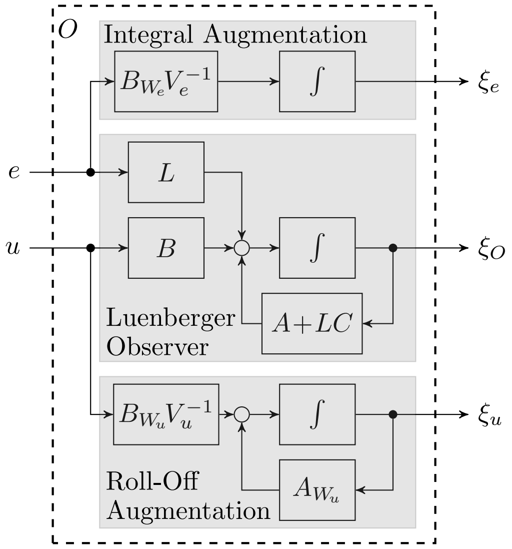

Fig. 3. Weight-augmented observer O.

The main result of Theis and Pfifer (2020) is summarized in the following Theorem. To simplify notation, a strictly proper plant ($D = 0$) as well as weights $W_e = I$ and $W_u = I$ are assumed.

Theorem 1. Let $\mathcal{P}$ and $\mathcal{Q}$ be given compact sets, let P be a given LPV system with $D = 0$, and let the weights W_e and W_u in Fig. 1 equal identity matrices of appropriate dimensions. Denote $\bar{B}_d = BV_d$, $\bar{B}_u = BV_u$, and $\bar{C}_e = V_e^{-1}C$. There exists an observer-based controller K as shown in Figs. 2 and 3 such that the induced $\mathcal{L}_2$-norm of the closed loop in Fig. 1 is less than γ if there exist continuously differentiable symmetric matrix functions $Z(\rho)\colon \mathcal{P} \to \mathbb{R}^{n_x \times n_x}$ and $Y(\rho)\colon \mathcal{P} \to \mathbb{R}^{n_x \times n_x}$ such that $\forall (p,q) \in \mathcal{P} \times \mathcal{Q}$

$$Z(p) > 0 \tag{6a}$$

$$\begin{bmatrix} \mathcal{Z}(p,q) & Z(p)\bar{B}_d(p) \\ \bar{B}_d^T(p)Z(p) & -I \end{bmatrix} < 0 \tag{6b}$$

$$\gamma > 1 \tag{7a}$$

$$Y(p) > 0 \tag{7b}$$

$$\begin{bmatrix} \mathcal{Y}(p,q) & -Y(p)\bar{C}_e^T(p) & -Z^{-1}(p)\bar{C}_e^T(p) \\ -\bar{C}_e(p)Y(p) & -\gamma I & I \\ -\bar{C}_e(p)Z^{-1}(p) & I & -\gamma I \end{bmatrix} < 0, \tag{7c}$$

with $\mathcal{Z}(p,q) = Z(p)A(p) + A^T(p)Z(p) + \sum_{i=1}^{n_\rho} \frac{\partial Z(p)}{\partial p_i} q_i - \bar{C}_e^T(p)\bar{C}_e(p)$ and $\mathcal{Y}(p,q) = Y(p)A^T(p) + A(p)Y(p) - \sum_{i=1}^{n_\rho} \frac{\partial Y(p)}{\partial p_i} q_i - \gamma \bar{B}_u(p)\bar{B}_u^T(p)$. The expression $Z > 0$ ($Z < 0$) denotes positive (negative) definiteness of Z.

Proof. The proof is only outlined here due to limited space. A detailed proof of the general weighted case is provided in Theis and Pfifer (2020). In essence, the condition (6) establishes the existence of a contractive left coprime factorization (see Prempain, 2006) and yields an observer gain $L(p) = -Z^{-1}(p)\,\bar{C}_e^T(p)\,V_e^{-1}(p)$. A state space coordinate transformation shows that condition (7) guarantees the existence of a state feedback gain $F(p) = -V_u(p)\,\bar{B}_u^T(p)\,Y^{-1}(p)$ for a generalized plant that includes the observer and represents the same performance specifications as Fig. 1. Finally, submultiplicativity of the induced $\mathcal{L}_2$-norm guarantees that γ is an upper bound on the performance of the closed-loop system. □

Condition (6) and (7) are coupled through Z in only one direction. Hence, they can be solved sequentially. First, a semidefinite program $\min_{X,Z(p)} \operatorname{trace}(X)$ s. t. $\left[\begin{smallmatrix} X & I \\ I & Z(p) \end{smallmatrix}\right] > 0$ and condition (6) is used to obtain Z and, respectively, the observer gain L. Then, a semidefinite program $\min_{\gamma,Y(p)} \gamma$ s. t. condition (7) is solved to obtain the state feedback gain F. Doing so replaces the SDP of the conventional output feedback synthesis with two smaller SDPs. As SDPs scale badly with the number of decision variables, solving the two smaller SDPs is much faster than solving the original problem.

3. ANTI-WINDUP COMPENSATION WITH DIFFERENTIAL IMPLEMENTATION

The purpose of anti-windup compensation is to prevent integrator states in the controller from building up when the control signal is saturated, e. g., due to actuator limits. When the integrator dynamics are lumped at the controller output as depicted in Fig. 4, anti-windup compensation is easily included. In this case, the controller output u equals the integrator state. It is then straightforward to manipulate this state as a function of the saturation level $\sigma = u - u_{\text{sat}}$, e. g. via backcalculation or integrator clamping (Åström and Hägglund, 2006). Backcalculation refers to proportional feedback of the saturation level to the integrator input. Integrator clamping denotes a logic that sets the integrator input to zero as long as $\sigma \neq 0$ and therefore holds the integrator state constant. Another popular variant is conditional integrator clamping which additionally considers directionality. That is, the integrator state is held constant only when both $\sigma \neq 0$ and $\operatorname{sign}(\sigma) = \operatorname{sign}(\dot{u})$. Such simple modifications do not increase controller complexity. In case the integrator is part of the controller dynamics, anti-windup compensation becomes severely more elaborate: For a generic dynamic LPV controller, the anti-windup compensator itself is, in general, LPV and has the same order as the controller (e. g. Lu et al., 2005).

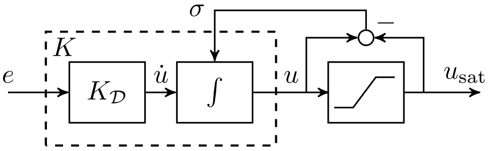

Fig. 4. Anti-windup compensation with integrator dynamics lumped at controller output.

Inspection of the observer-based controller (see Figs. 2 and 3) shows that it is not in the form of Fig. 4. Hence, simple anti-windup schemes cannot be directly applied to the proposed controller. However, the presence of integrator dynamics at the output can be enforced by a differential implementation, see e. g. Osterhuber et al. (2004). The differential implementation paradigm states that the controller provides a differential control signal $\dot{u}$ and an integrator at the output calculates u. A controller in differential implementation is hence in the form of Fig. 4 and thus desirable for simple anti-windup compensation. One way of implementing a differential form for general state space controllers is the $\mathcal{D}$-implementation, originally developed by Kaminer et al. (1995) as a means to circumvent excitation of so-called hidden couplings in gain-scheduled controllers (cf. Nichols et al., 1993; Shamma and Cloutier, 1993). The $\mathcal{D}$-implementation can be interpreted as a clever realization of $\frac{1}{s}\,K\,s$. That is, the error signal is differentiated at the input of the controller and an integrator is placed at the output of the controller, cf. Sedlmair et al. (2019a). In other words, $K_\mathcal{D} = K\,s$ in Fig. 4. For linear time-invariant controllers, the approach is straightforward. For time-varying controllers, however, $\mathcal{D}$-implementation is an ad hoc modification that does not preserve the input-output behavior of the controller (cf. also Mehendale and Grigoriadis, 2004, 2006).

In the following, it is shown how the structure of the observer-based controller can be exploited to achieve the form of Fig. 4 such that a simple anti-windup scheme can be implemented. The proposed approach is based on an *exact* differential implementation of the observer-based controller followed by an approximation commonly used in LPV control: neglecting the scheduling parameter variation rate. For the observer-based controller, the control signal is $u = F(\rho)\,\xi$. Differentiation with respect to time yields

$$\dot{u} = F(\rho)\,\dot{\xi} + \underbrace{\sum_{i=1}^{n_\rho} \frac{\partial F(\rho)}{\partial \rho_i}\,\dot{\rho}_i\,\xi}_{\partial F(\rho,\dot{\rho})}. \qquad (8)$$

The differential input is a function of both the controller state ξ and its time-derivative $\dot{\xi}$. This dependence does not increase controller complexity, as the augmented observer is easily modified such that it provides $\dot{\xi}$ in addition to ξ, see Fig. 5. Thus, the observer-based controller is *exactly* represented by the implementation in Fig. 6. Note, however, that there is now an explicit dependence on the scheduling parameter variation rate $\dot{\rho}$ through ∂F.

The implementation in Fig. 6 still has a pure integrator (for ξ_e) in the observer and therefore does not lump all integrator dynamics at the output. Thus, it is not suitable for simple anti-windup compensation. Note that the observer state ξ is multiplied only by ∂F, see Fig. 6. If either F is parameter-independent or the scheduling parameter variation is assumed to be slow ($\dot{\rho} \approx 0$), the result is $\partial F = 0$ and the dotted elements in Fig. 5 are no longer required. Removing said dotted parts results in an observer-based LPV controller as shown in Fig. 7. Anti-windup compensation is then easily added. Note that the implementation according to Fig. 7 is only an approximation of the originally designed controller when $F(\rho) \neq$ *const.* and care has to be taken whether the approximation is justified. Nevertheless, it should be emphasized that rate dependence is often ignored in the implementation of conventional LPV output feedback controllers. Even then, the form of Fig. 7 cannot, in general, be obtained for such controllers.

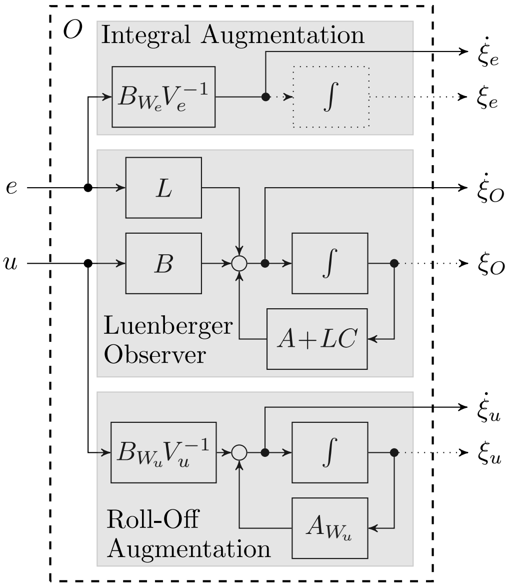

Fig. 5. Weight-augmented observer with state derivative output.

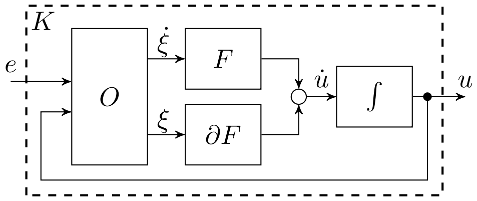

Fig. 6. Observer-based controller in exact differential implementation.

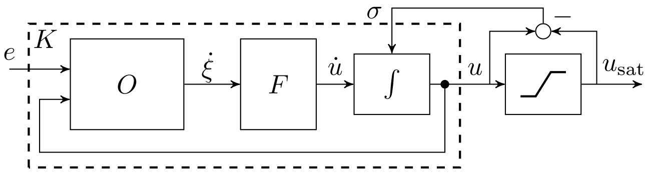

Fig. 7. Approximate observer-based controller with anti-windup compensation.

4. CONTROL DESIGN EXAMPLE

The following design example demonstrates the applicability of the anti-windup-compensated observer-based LPV controller for a flight control application. The control objective is to achieve fast tracking of commands for the vertical acceleration. Control of the vertical acceleration is a common way of realizing longitudinal control for aircraft. The unmanned low-cost testing research aircraft (ULTRA) Extra, depicted in Fig. 8, is an unmanned replica of the aerobatic aircraft Extra 330 ML with a scale of 1:2.5. The ULTRA Extra has a total mass of 24.6 kg and a wingspan of 3.10 m. An extensive flight test campaign with a total of 148 identification maneuvers was performed in order to identify aerodynamic parameters for a nonlinear six degrees-of-freedom gray-box model (Sedlmair et al., 2019b). The dynamics of the control surface servos and sensors where identified on the component level.

Fig. 8. Unmanned aircraft ULTRA Extra.

4.1 Control Design and Synthesis

The vertical acceleration and the pitch rate, both measured at the center of gravity, are used as feedback signals. The elevator is used as the control effector such that a multi-input-single-output controller results. The nonlinear model of the ULTRA Extra is linearized for straight and level flight at airspeeds $V_\infty \in \{18, 20, 25, 30, 35, 40, 42\}$ m/s to form a grid-based LPV model with $\rho = V_\infty$. For controller synthesis, the LPV model is reduced to a second-order short period model. This short period model is augmented with a fourth-order model representing parasitic effects such as servo actuator dynamics, sensor dynamics, signal filtering, and an input delay of 53 ms.

The mixed sensitivity formulation (3) described in Section 2.2 is used for control design. Parameter-independent weights W_e and W_u are used to provide common performance specifications throughout the flight envelope. The weight W_e is selected to have integral behavior up to a tracking bandwidth of 2.7 rad/s for the vertical acceleration. In order to limit the peak sensitivity to a factor of two, a gain of 0.5 is selected beyond this frequency. With the same rationale, a constant gain of 0.5 is chosen to weight the pitch rate. The weight W_u is selected with unit gain up to 30 rad/s and a slope of +20 dB between 30 rad/s and 300 rad/s. This ensures controller roll-off and reduces noise sensitivity. Parameter-dependent static weights V are used for tuning. Initially, the weight $V_e(\rho)$ is selected such that the ratios of the steady-state responses in vertical acceleration and pitch rate due to a step input to the open-loop plant model are reflected. The weight $V_u(\rho)$ is then selected such that it varies from 25° at low airspeeds to 3° at high airspeeds to account for the variation in control surface effectiveness. Finally, the weight V_d is tuned to $0.2\,V_u$ to represent 20% actuator uncertainty.

Affine basis functions for $Z(\rho)$ and $Y(\rho)$ are used to arrive at a finite dimensional formulation for Theorem 1. The SDP solver `mincx`, part of the Matlab Robust Control Toolbox (Balas et al., 2019), is used to obtain feasible $Z(\rho)$ and $Y(\rho)$ from which the observer and state feedback gains are calculated. A 10 % suboptimal solution is used in order to improve numerical behavior, cf. Balas et al. (2015). The resulting F and L are functions of the airspeed.

4.2 Simulation Results

Controller performance is evaluated using a nonlinear high-fidelity simulation model of the ULTRA Extra aircraft. The model includes actuator dynamics with rate limits and saturation, time delay, and backlash. Channel-specific measurement noise, transport delays, signal filters, quantization effects, and rate transitions are also included. Figure 9 compares simulation results for a vertical acceleration tracking task with the exact implementation of Fig. 6 and the approximation of Fig. 7. The simulation starts in a 1 g straight and level flight with an airspeed of 38 m/s. After 1 second, a pull-up command with 4 g is issued for 1.5 s. Then, the reference is switched to a -1 g-pull-down for another 1.5 s before returning to 1 g.

Both implementations yield very similar results: fast and well-damped responses with excellent transient behavior. Note that the 4 g-pull-up maneuver is quite aggressive. It leads to a sharp drop in airspeed from 38 m/s to around 25 m/s in 3 s. During the time where the airspeed varies, no steady state is reached and the controller cannot track the desired acceleration of 4 g exactly. The exact implementation shows a slightly lower tracking error here, which is achieved by continuously increasing elevator deflection. The approximate implementation issues less deflection and lacks the build-up characteristic. This difference is the result of neglecting the rate-depended term ∂F. As the acceleration of the aircraft and not its attitude is the controlled variable, the slight difference in the acceleration profiles of the two implementations integrates over time. In other words, the aircraft's attitude is different at the end of the two simulations. The angle of attack plot illustrates this: The exact implementation results in a steady state with about 5° angle of attack, whereas the approximate implementation results in about 3°. Hence, the airspeed required to achieve 1 g steady-state flight also differs, which explains the difference in the airspeed profiles. In summary, the error introduced by the approximate implementation is small for the considered application and the controller functions as expected.

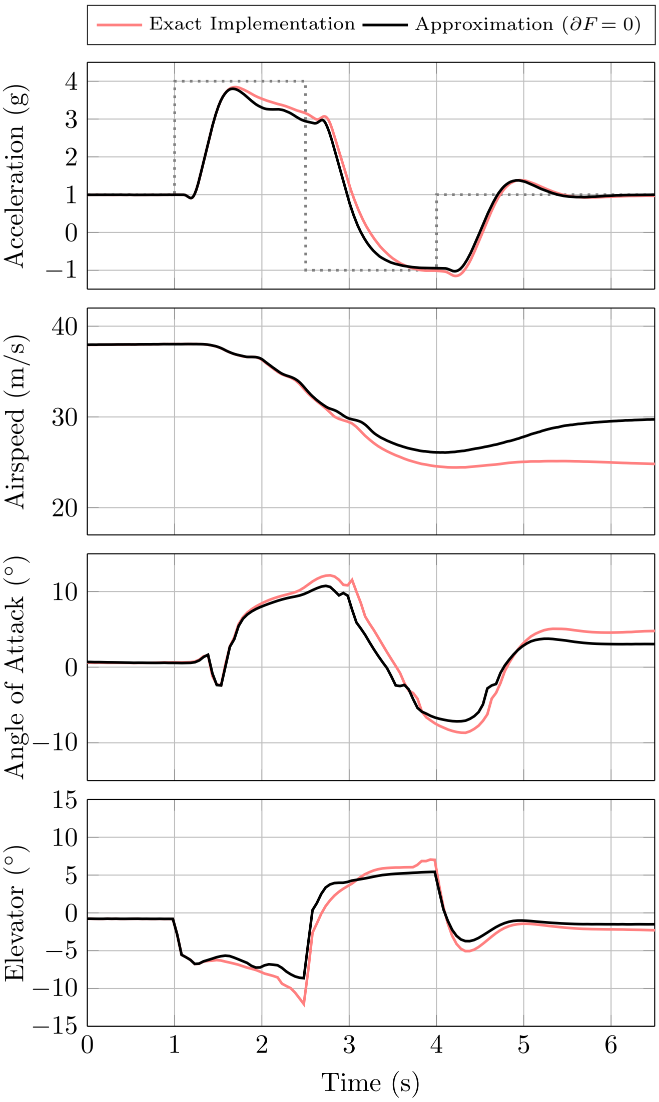

Fig. 9. Simulation of vertical acceleration doublet.

In order to demonstrate anti-windup compensation, the elevator command signal is saturated at ±5°. A simple conditional integrator clamping logic as described by Åström and Hägglund (2006) is used. Figure 10 shows a simulation of the same doublet maneuver as before, but with saturation. The available control action is not sufficient for tracking the first step and the controller output saturates. The benefit of anti-windup compensation becomes evident at simulation time $t = 2.5\,\mathrm{s}$, where the reference is changed. Without anti-windup compensation, the controller remains in saturation for an additional 0.2 s. This is the typical delayed response associated with the time required to wind down the integrator state after saturation occurs. In contrast, the controller with anti-windup compensation reacts immediately.

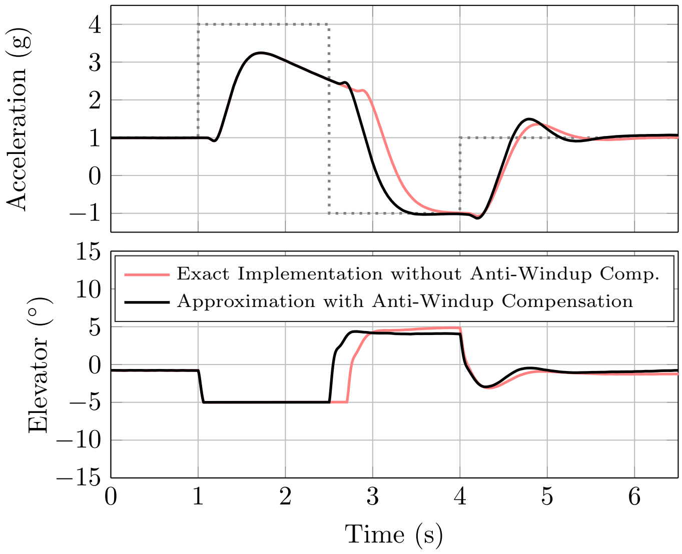

Fig. 10. Simulation of vertical acceleration doublet with reduced saturation limits.

5. CONCLUSION

The paper presents a novel differential implementation for observer-based state space controllers. This implementation makes it possible to combine simple anti-windup compensation strategies and LPV control. As such, the paper contributes an important element for practical LPV control since LPV anti-windup compensation usually increases controller complexity. Applicability of the method is demonstrated on the flight-test-validated high-fidelity model of an unmanned aircraft in nonlinear simulation.

REFERENCES

Apkarian, P. and Gahinet, P. (1995). A convex characterization of gain-scheduled H_∞ controllers. *IEEE Trans. Autom. Control*, 40(5), 853–864. doi:10.1109/9.384219.

Apkarian, P., Gahinet, P., and Becker, G. (1995). Self-scheduled H_∞ control of linear parameter-varying systems: A design example. *Automatica*, 31, 1251–1261. doi:10.1016/0005-1098(95)00038-X.

Åström, K. and Hägglund, T. (2006). *Advanced PID Control*. Instrumentation, Systems & Automation Society.

Balas, G., Chiang, R., Packard, A., and Safonov, M. (2019). Robust control toolbox R2019a. Mathworks, Inc.

Balas, G., Hjartarson, A., Packard, A., and Seiler, P. (2015). *LPVTools: A Toolbox For Modeling, Analysis, and Synthesis of Parameter Varying Control Systems.* MuSyn, Minneapolis, MN. Software and User's Manual.

Becker, G. and Packard, A. (1994). Robust performance of linear parametrically varying systems using parametrically dependent linear feedback. *Syst. Control Lett.*, 23(3), 205–215. doi:10.1016/0167-6911(94)90006-x.

Bennani, S., Willemsen, D., and Scherer, C. (1998). Robust control of linear parametrically varying systems with bounded rates. *J. Guid. Control Dyn.*, 21(6), 916–922. doi:10.2514/2.4325.

Hjartarson, A., Seiler, P., and Packard, A. (2015). LPV-Tools: A toolbox for modeling, analysis, and synthesis of parameter varying control systems. *IFAC- PapersOnLine*, 48(26), 139–145. doi:10.1016/j.ifacol.2015.11.127.

Kaminer, I., Pascoal, A.M., Khargonekar, P.P., and Coleman, E.E. (1995). A velocity algorithm for the implementation of gain-scheduled controllers. *Automatica*, 31(8), 1185–1191. doi:10.1016/0005-1098(95)00026-s.

Lu, B., Wu, F., and Kim, S. (2005). Linear parameter-varying antiwindup compensation for enhanced flight control performance. *J. Guid., Control, Dyn.*, 28(3), 494–505. doi:10.2514/1.4952.

Mehendale, C. and Grigoriadis, K. (2004). A new approach to LPV gain-scheduling design and implementation. In *IEEE Conf. Decision Cont.*, 2942–2947. doi:10.1109/cdc.2004.1428914.

Mehendale, C. and Grigoriadis, K. (2006). Performance of LPV gain-scheduled systems. In *American Control Conf.*, 2915–2920. doi:10.1109/acc.2006.1657162.

Nichols, R., Reichert, R., and Rugh, W. (1993). Gain scheduling for H_∞ controllers: A flight control example. *IEEE Trans. Control Syst. Technology*, 1(2), 69–79. doi:10.1109/87.238400.

Osterhuber, R., Hanel, M., and Hammon, R. (2004). Realization of the Eurofighter 2000 primary lateral/directional flight control laws with differential PI-algorithm. In *AIAA Guid., Navigation, Control Conf.* doi:10.2514/6.2004-4751.

Prempain, E. (2006). On coprime factors for parameter-dependent systems. *45th IEEE Conf. Decision Control*, 5796–5800. doi:10.1109/cdc.2006.376773.

Prempain, E., Turner, M., and Postlethwaite, I. (2009). Coprime factor based anti-windup synthesis for parameter-dependent systems. *Syst. Control Lett.*, 58(12), 810–817. doi:10.1016/j.sysconle.2009.09.002.

Sedlmair, N., Theis, J., and Thielecke, F. (2019a). Automatic three-point landing of a UAV with H_∞-control in d-implementation. *IFAC-PapersOnLine*, 52(12), 316–321. doi:10.1016/j.ifacol.2019.11.262.

Sedlmair, N., Theis, J., and Thielecke, F. (2019b). Design and experimental validation of UAV control laws – 3D spline-path-following and easy-handling remote control. In *5th CEAS Conf. Guid., Navigation, Control.*

Shamma, J.S. and Cloutier, J.R. (1993). Gain-scheduled missile autopilot design using linear parameter varying transformations. *J. Guid., Control, Dyn.*, 16(2), 256–263. doi:10.2514/3.20997.

Skogestad, S. and Postlethwaite, I. (2005). *Multivariable Feedback Control.* Prentice Hall, Upper Saddle River, NJ.

Theis, J., Ossmann, D., Thielecke, F., and Pfifer, H. (2018). Robust autopilot design for landing a large civil aircraft in crosswind. *Control Engineering Practice*, 76, 54–64. doi:10.1016/j.conengprac.2018.04.010.

Theis, J. and Pfifer, H. (2020). Observer-based synthesis of linear parameter-varying mixed sensitivity controllers. *Int. J. Robust Nonlin. Control.* doi:10.1002/rnc.5038.

Theis, J., Pfifer, H., and Seiler, P. (2020). Robust modal damping control for active flutter suppression. *J. Guid., Control, Dyn.* doi:10.2514/1.G004846.

Wu, F., Grigoriadis, K.M., and Packard, A. (2000). Anti-windup controller design using linear parameter-varying control methods. *Int. J. Control*, 73(12), 1104–1114. doi:10.1080/002071700414211.

Wu, F., Yang, X.H., Packard, A., and Becker, G. (1996). Induced $\mathcal{L}_2$-norm control for LPV systems with bounded parameter variation rates. *Int. J. Robust Nonlin. Control*, 6(9-10), 983–998.